

Stability of synchronization in a multi-cellular system

SUMA GHOSH^{1(a)}, GOVINDAN RANGARAJAN¹ and SOMDATTA SINHA^{2(b)}

¹ Department of Mathematics, Indian Institute of Science - Bangalore, India

² Centre for Cellular and Molecular Biology (CSIR) - Hyderabad, India

received 4 August 2010; accepted in final form 8 November 2010

published online 10 December 2010

PACS 05.45.Xt – Synchronization; coupled oscillators

PACS 87.10.Ed – Ordinary differential equations (ODE), partial differential equations (PDE), integrodifferential models

PACS 87.18.Gh – Cell-cell communication; collective behavior of motile cells

Abstract – Networks of biochemical reactions regulated by positive- and negative-feedback processes underlie functional dynamics in single cells. Synchronization of dynamics in the constituent cells is a hallmark of collective behavior in multi-cellular biological systems. Stability of the synchronized state is required for robust functioning of the multi-cell system in the face of noise and perturbation. Yet, the ability to respond to signals and change functional dynamics are also important features during development, disease, and evolution in living systems. In this paper, using a coupled multi-cell system model, we investigate the role of system size, coupling strength and its topology on the synchronization of the collective dynamics and its stability. Even though different coupling topologies lead to synchronization of collective dynamics, diffusive coupling through the end product of the pathway does not confer stability to the synchronized state. The results are discussed with a view to their prevalence in biological systems.

Copyright © EPLA, 2010

Introduction. – The emergence of collective behavior is an important step in the evolution of multi-cellular life from single cells. In single cells, coordinated cellular functions are performed by networks of biochemical reactions, regulated by positive- and negative-feedback processes. These cells communicate through exchange of chemicals and signals, and cooperate to work together in the multi-cellular environment (*e.g.*, tissues and organisms). Understanding how the synchronized collective behavior of multi-cellular systems evolves depending on local intra-cellular properties and global features (such as, environment, system size, and interaction strength/topology), and the robustness of such behavior in response to noise in view of adaptability of biological systems are some of the most important questions in biology today [1].

Synchronization is a well-known collective phenomenon in various multi-component physical and biological systems [2]. The exchange of information (coupling) among the components can be global (all-to-all) or local (nearest neighbors). Depending on various intrinsic and extrinsic factors, the coupled dynamics can exhibit different types of synchronization such as complete synchronization, phase and lag synchronization, intermittent phase

synchronization, etc. Phase synchronization is the weakest form of synchronization and is typically observed when coupling is weak. As coupling strengths increase, more ordered stages of synchronized dynamics are obtained, culminating in the strongest form of synchronization—the complete synchronization. When phase entrainment is lost and regained intermittently in a coupled system, it is called intermittent phase synchronization [2].

An essential prerequisite for understanding the synchronization of a coupled system is to know the bounds on the coupling strengths which ensure the stability of the synchronized state. The stability of the synchronized state is hard to study mathematically for phase synchronization whereas it is relatively easy for complete synchronization. Many attempts have been made (see the references quoted in [3]) to obtain such stability conditions for physical systems—typically for small network sizes or for specific types of couplings. In order to ensure stability of the synchronized state for a general coupling scheme, analytical bounds were obtained on coupling strengths [3,4] following the notion of the master stability function [5]. Physical systems were the primary focus in these studies. For biological systems, such as tissues and organized cell assemblies, it is not clear if the stability of the synchronized state is useful or detrimental to its functions. On the one hand, synchronization is necessary for the proper functioning of the system in the face of both internal and

^(a)Present address: Department of Mathematics and Statistics, York University - Toronto, Canada.

^(b)E-mail: sinha@ccmb.res.in

external environmental perturbations; on the other, changes in functional states during development or disease require sensitivity to external stimuli leading to transient or long-term changes in functional dynamics in the system [6].

In this paper, we investigate conditions under which synchronization and its stability are achieved and maintained in a model multi-cellular system represented by a ring of coupled cells. Each cell incorporates a three-step model biochemical network of positive- and negative-feedback processes, which is a simple and general scheme representing a large variety of functional dynamics observed in cellular systems [7]. We consider two coupling schemes —diffusive coupling through all three substrates of the reaction pathway to their nearest neighbors, and the more commonly observed coupling through diffusion of the end product alone. We derive analytical conditions for stability and validate numerically, for different coupling schemes and system sizes, using the master stability function approach. The degree of synchronization in the coupled cells is also studied. Our study gives indications of how system sizes and variation in cell-cell interactions (coupling) and their topology play important roles in both robustness and sensitivity of the synchronized functional state in multi-cellular systems.

Model and methods. —

Multi-cell system. — We consider a one-dimensional lattice of identical cells with periodic boundary conditions (*e.g.*, cellular arrangement in plant roots) [8], where each cell incorporates a model three-step biochemical pathway regulated by end product inhibition of the first substrate (negative feedback), and autocatalytic activation of the end product through an allosteric enzyme (positive feedback). Each cell is coupled to its two nearest neighbors through diffusion of all three substrates of the reaction pathway. The dynamical evolution of the pathway in the coupled cells is described by

$$\frac{dx_j}{dt} = f(z_j) - \kappa x_j + \frac{\epsilon_1}{2}(x_{j+1} + x_{j-1} - 2x_j), \quad (1)$$

$$\frac{dy_j}{dt} = x_j - g(y_j, z_j) + \frac{\epsilon_2}{2}(y_{j+1} + y_{j-1} - 2y_j), \quad (2)$$

$$\frac{dz_j}{dt} = g(y_j, z_j) - qz_j + \frac{\epsilon_3}{2}(z_{j+1} + z_{j-1} - 2z_j), \quad (3)$$

where x, y, z are the normalized concentrations of the substrates, $\epsilon_1, \epsilon_2, \epsilon_3$ are the diffusive coupling strengths of the three substrates, and j the cell number ranging from 1 to N . The parameters κ and q are the rates of degradation of the first substrate and end product, respectively. The nonlinear functions $f(z)$ and $g(y, z)$ represent the negative- and positive-feedback processes given by

$$f(z) = \frac{1}{1+z^4}, \quad g(y, z) = \frac{Ty(1+y)(1+z)^2}{L+(1+y)^2(1+z)^2}, \quad (4)$$

where, L and T are related to allosteric constant and maximum velocity of the enzyme. $L = 10^6$ and $T = 10$ for

typical allosteric enzymes involved in cellular processes possessing similar positive- and negative-feedback mechanisms, which exhibit sustained oscillations in Glycolysis, cyclic AMP oscillations, neuronal excitability and oscillations, mitosis in eukaryotic cells, and circadian rhythms [7,9]. Earlier studies have shown that this model cell can exhibit a range of dynamics —equilibrium, limit cycle, period doubling, bi-rhythmicity, complex oscillations, and chaos, along with sensitivity to external noise—with variation of parameters κ and q [10,11]. For all studies presented here, $\epsilon_1 = \epsilon_2 = \epsilon_3 = \epsilon$, and for coupling through the diffusion of the end product (z) alone, $\epsilon_1 = \epsilon_2 = 0$.

Numerical simulations were performed in FORTRAN using the fourth-order Runge-Kutta method for $t \sim 10^7$, and only long-term dynamics are shown. Thus, we have not probed the transient dynamics that may precede the final synchronized state as was shown for the quorum-sensing type of coupling [12]. The Lyapunov exponents were calculated using Wolf's algorithm [13]. The degree of synchronization was quantified using the synchronization order parameter R [14]. R is defined as the ratio of the standard deviation of the time series of the average signal to the standard deviation of the individual signal. The z component of R is defined as

$$R_z = \frac{\langle M(t)^2 \rangle - \langle M(t) \rangle^2}{[\langle z_i^2 \rangle - \langle z_i \rangle^2]}. \quad (5)$$

Here, $\langle \rangle$ denotes the time average, and $[]$ represents the average over all cells. $M(t)$ is the spatial average of z over N cells at time t . R_x and R_y can be similarly defined. $R \approx 0$ in the unsynchronized, and $R \approx 1$ in the synchronized state.

Results. — This study was done on single cells with $\kappa = 0.003$ and $q = 0.1$ exhibiting chaotic dynamics (Lyapunov exponents: 0.00358, 0.00002, -0.01681), and fig. 1(a) shows the $(y-z)$ phase portrait. Figure 1(b) shows the superposition of the time series of end product z in 50 cells with no cell-cell interactions. The temporal behavior of these uncoupled cells is seen to be totally uncorrelated.

Dynamics of coupled multi-cellular system. — The dynamics of the coupled multi-cellular system (cf. eqs. (1)–(3)) is governed by two main parameters: the number of cells N (ring size), and the coupling strength ϵ . Here we present the collective dynamics of the cells in the ring for various values of N and ϵ .

Role of system size (N) and coupling strength (ϵ): — We investigated the local (single cell) as well as the global (all cells in the ring) dynamics of the multi-cellular system by varying the number of cells from $N = 10$ to 110 at a fixed coupling strength $\epsilon = 0.7$ (table 1 and fig. 1(c)–(f)). Rings of $10 \leq N \leq 50$ exhibit complete chaotic synchronization (CS) to its local chaotic behavior. Superposition of the time series of z from 50 cells in fig. 1(c) shows a single trajectory indicating that the coupled cells are in

Table 1: Variation of local and global dynamics with size of the lattice (N). Notations: CH, chaos; CS, complete synchronization; PS, phase synchronization; IPS, intermittent phase synchronization; P2, period-2 cycle; P4, period-4 cycle.

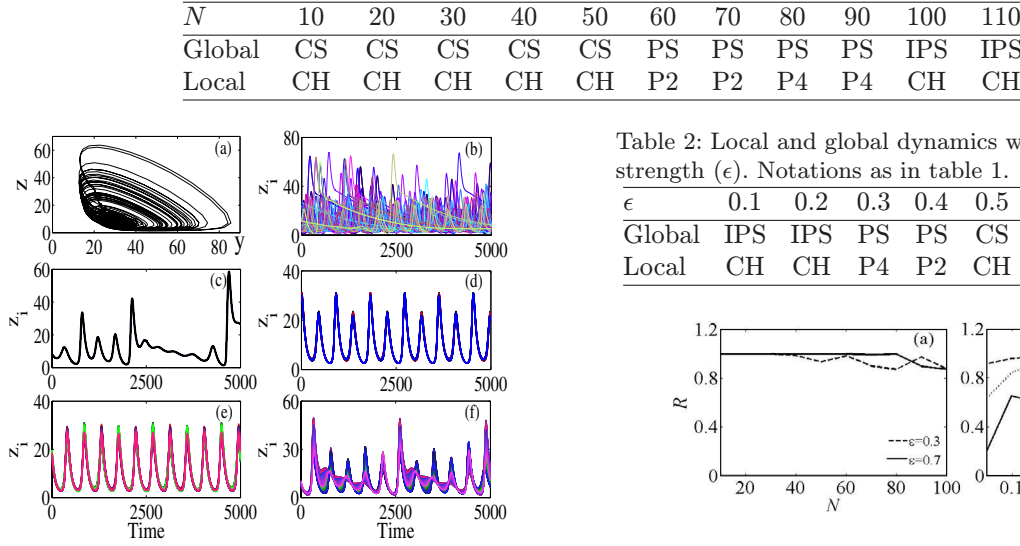


Fig. 1: (Colour on-line) Global and local dynamics exhibited by the end product z in the ring of cells of different sizes. (a) Chaotic dynamics in an isolated single cell; (b) chaotic dynamics in 50 uncoupled cells. Dynamics in coupled cells ($\epsilon = 0.7$): (c) CS for $N = 50$; (d) PS (local and global P2 dynamics) for $N = 60$; (e) PS with phase lag (local P4) for $N = 80$, and (f) IPS (local chaotic) for $N = 110$. See text for details.

complete synchronization. Thus, the global dynamics of the multi-cell system coincides perfectly with the inherent and local dynamics of the cells (fig. 1(a)). This is in contrast to earlier work [8] based on coupling through z only, where, complete CS was obtained only for small lattices. Thus diffusive coupling across all three substrates among the cells, induces complete synchronization in rings of larger sizes.

As given in table 1, a further increase in system sizes ($60 \leq N \leq 90$) influences both the local and global behavior of the ring of cells. The local chaotic dynamics in individual cells are completely suppressed to regular period-2 and period-4 (P2, P4) oscillations, and the emergent global dynamics is phase synchronized (PS). For $N = 60\text{--}70$, both individual cells and the in-phase synchronized multi-cellular system exhibits stable P2 oscillations (fig. 1(d)). In contrast, for $N = 80\text{--}90$, the constituent cells exhibit P4 dynamics, but the global dynamics of the lattice shows a repeating pattern of two higher peaks and two lower peaks (fig. 1(e)). This arises because the peaks of the P4 oscillations in all cells do not overlap at the same time, and have a fixed phase lag of one-fourth. Thus, the local and global dynamics in the multi-cellular system are quite different from that of the uncoupled system, and the size of the system can influence both the constituent cells' local dynamics and their collective behavior.

Increasing the system size ($100 \leq N \leq 110$) leads to intermittent phase synchronization (IPS) in the ring of cells (fig. 1(f)), where the superimposed time series corresponding to each cell are not perfectly correlated. The

Table 2: Local and global dynamics with variation in coupling strength (ϵ). Notations as in table 1.

ϵ	0.1	0.2	0.3	0.4	0.5	0.6	0.7	0.8	0.9
Global	IPS	IPS	PS	PS	CS	CS	CS	CS	CS
Local	CH	CH	P4	P2	CH	CH	CH	CH	CH

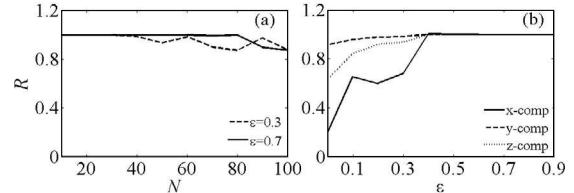


Fig. 2: Synchronization order parameter R : (a) R_z with N for $\epsilon = 0.3$ and 0.7 ; (b) R with ϵ for $N = 50$.

local dynamics of all cells in the ring remains chaotic. This behavior continues to dominate at larger systems sizes ($N = 500$). In general, for the same coupling strength, increase in system size prevents CS.

The strength of coupling also plays a significant role in influencing the interplay between the local and global dynamics in the multi-cellular system. Table 2 lists the local and global dynamics in the ring of cells ($N = 50$) for coupling strengths $0.1 \leq \epsilon \leq 0.9$. It is clear that higher coupling strength ($0.5 \leq \epsilon \leq 0.9$) is required for global CS, keeping the individual cell dynamics chaotic. Suppression of chaos is observed both at local and global level for medium values of ϵ ($0.3 \leq \epsilon \leq 0.4$). At lower ϵ ($0.1 \leq \epsilon \leq 0.2$), the cells remain chaotic and IPS is observed in global dynamics. Thus, when diffusion occurs in all substrates, a higher coupling strength is required for this multi-cellular system to remain completely synchronized. As N is increased, CS happens only at higher ϵ , with PS and IPS dominating for $N \geq 80$.

Quantitative study of synchronization. The degree of synchronization in the coupled multi-cellular system (with all-component coupling) for different N and ϵ is measured using R (eq. (5)). Figure 2(a) shows R_z for different ring sizes ($10 \leq N \leq 100$) at two coupling strengths $\epsilon = 0.3$ and 0.7 . For $\epsilon = 0.7$, the coupled cells shows complete synchrony ($R_z > 0.99$) in the range $10 < N < 80$ where the global dynamics is in CS or PS state (cf. table 1). At lower coupling strength ($\epsilon = 0.3$), the system shows CS only for $10 < N < 30$. Thus, there is a general trend of decreasing level of synchronization with increasing system size at lower cell-cell interaction strengths. Figure 2(b) shows the variation of R_x , R_y and R_z with increasing ϵ for a fixed ring size, $N = 50$. Here the cells show complete synchronization ($R = 1$) for all three components x, y, z for coupling strengths $0.4 < \epsilon < 1$. The y and z

components also show a high synchronization order ($R > 0.9$) in the range $0.2 < \epsilon < 0.4$ where the system shows phase synchronization (cf. table 2).

Stability of synchronization.

Analytical deduction: We now derive an analytic criterion for stability of the synchronized state following the approach given in refs. [3–5]. Equations (1)–(3) of the coupled cell model can be written in the form

$$\dot{X} = I_N \otimes F(X) + \frac{\epsilon}{2} G \otimes H(X). \quad (6)$$

Here $X = (X^1, X^2, \dots, X^N)^T$; $X^j = (x^j, y^j, z^j)$, $j = 1, 2, \dots, N$; I_N is the $N \times N$ identity matrix; $F(X) = (F(X^1), F(X^2), \dots, F(X^N))^T$, where each $F(X^j)$ represents the single cell dynamics; $H(X) = X$ and finally the (diffusive) coupling matrix G whose non-zero elements are given by $G_{ii} = -2$, $G_{i,i+1} = G_{i+1,i} = 1$ for $i = 1, 2, \dots, N$ (with the understanding that the indices cannot exceed N).

To study the linear stability of the synchronized state, we need the variational (linearized) equation corresponding to eq. (6). Denoting the variation on the j -th cell by $\xi^j = (\delta x^j, \delta y^j, \delta z^j)$ and the collection of variations by $\xi = (\xi^1, \xi^2, \dots, \xi^N)$, the variational equation corresponding to eq. (6) can be written as

$$\dot{\xi} = \left[I_N \otimes DF + \frac{\epsilon}{2} G \otimes I_3 \right] \xi \quad (7)$$

where DF represents the variational matrix for each cell. For linear stability of the synchronized state, we need to consider only those variations that are transverse to the synchronization manifold, and all these should damp out. By diagonalizing G , we get a block-diagonalized variational form of eq. (7) where each block has the form (see [5])

$$\dot{\xi}_k = \left(DF + \frac{\epsilon}{2} \gamma_k I_3 \right) \xi_k \quad (8)$$

Here $\gamma_k = -4 \sin^2 \frac{\pi k}{N}$, $k = 0, 1, 2, \dots, N-1$ is the k -th eigenvalue of G .

For $k = 0$ we have the variational equation for motion on the synchronization manifold ($\gamma_0 = 0$). For stability, variations transverse to this manifold are required, and these are given by eq. (8) with $k \neq 0$. For the transverse variations to damp out, the corresponding transverse Lyapunov exponents (LE) should be negative. One can calculate these transverse LE from eq. (8) for each $k \neq 0$. These transverse LE (denoted by λ_i^k) are related to the LE h_i ($i = 1, 2, 3$) of the single-cell model ($\epsilon_1 = \epsilon_2 = \epsilon_3 = 0$ in eqs. (1)–(3)), and to the eigenvalues of the coupling matrix G by

$$\lambda_i^k = h_i - 4 \left(\frac{\epsilon}{2} \right) \sin^2 \frac{\pi k}{N}, \quad k = 1, 2, \dots, (N-1); i = 1, 2, 3. \quad (9)$$

All these transverse LE are negative if the maximum Lyapunov exponent is less than zero. This gives $\lambda_{max}^k = h_{max} - 2\epsilon \sin^2 \frac{\pi k}{N} < 0$, where h_{max} denotes the maximum

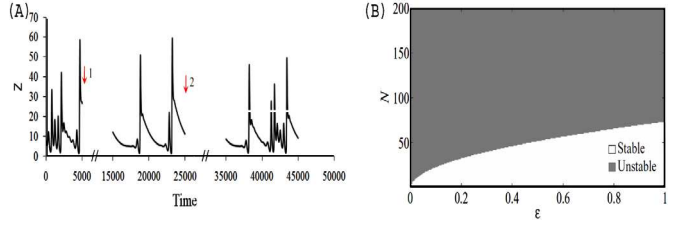


Fig. 3: (Colour on-line) (A) Dynamics of z of 50 coupled cells after perturbation at two time points (arrows 1 and 2). $\epsilon = 0.7$. (B) Stability region of synchronization for different (N) and ϵ .

LE of the single-cell model. Since $\sin^2 \frac{\pi k}{N}$ is smallest for $k = 1$, we get the final stability condition for synchronization to be

$$h_{max} < 2\epsilon \sin^2 \frac{\pi k}{N}. \quad (10)$$

The above results are valid for the specific diffusive coupling matrix G given earlier. For a general symmetric coupling, the master stability equation [15] is given by

$$\dot{\eta} = [DF + \alpha I_3]\eta, \quad (11)$$

where η denotes the variation and α is a real number parameterizing the eigenvalues of a general symmetric matrix G . For each α , one can numerically obtain λ_{max} . The values of α where $\lambda_{max} < 0$ constitute the stability region in the λ_{max} vs. α plot. For a specific symmetric matrix G , if all its eigenvalues fall within the stability region, the corresponding synchronized state will be stable. For more general couplings, the condition for stability may be derived by combining the master stability function with the Gershgorin disc theory [3,4].

Numerical verification: To demonstrate the stability of the complete chaotic synchronization (CS) state in terms of its sensitivity to external perturbations, the coupled ring of cells at the CS state ($N = 50$, $\epsilon = 0.7$) is perturbed by externally adding an instantaneous perturbation $z_{pert} = 2$ (arrow 1 in fig. 3(A)) to all the cells, and their time evolution studied numerically. Then the system is allowed to evolve for a long period before applying the perturbation second time (arrow 2). The long-term dynamics of this doubly perturbed system is seen to be still in the CS state, which is indicative of stability of the synchronized state. The behavior is similar at higher perturbation $z_{pert} = 10$ (not shown).

To find the regions of stability of the synchronized state for different N and ϵ , we study the stability condition given in eq. (10) which is valid for diffusive coupling. From (10), h_{max} is found numerically for the single-cell model for $\kappa = 0.003$, and the Lyapunov exponents calculated. Depending on the value of h_{max} , one can predict the upper bound of N , for a given ϵ , or the minimum ϵ needed for a given N , when the system is in a stable CS state. The stability plot is shown in fig. 3(B). It is clear from the figure that for a fixed N , a minimum ϵ is needed for the coupled system to enter into the stable synchronized state region. For example, for ring size $N = 50$, the minimum coupling

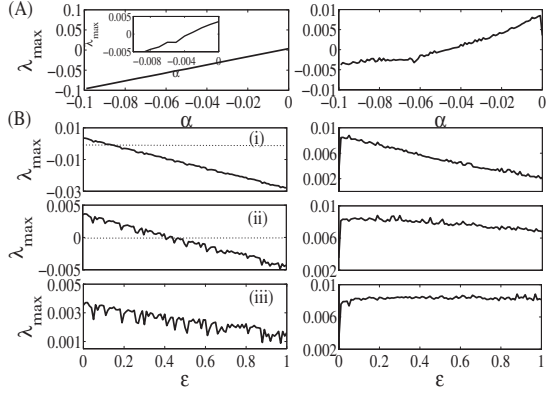


Fig. 4: (A) Maximum Lyapunov exponent (λ_{max}) from the master stability equation for all-component coupling (left column), z -component only (right column), for an arbitrary symmetric coupling. (B) Maximum transverse Lyapunov exponent for ring sizes $N = 25$ (i), $N = 50$ (ii) and $N = 100$ (iii), as a function of ϵ , for nearest-neighbour coupling through all components (left column) and z -component (right column).

strength needed is $\epsilon \approx 0.45$ for the synchronization state to be stable. With increase in ϵ , the region of stability for a fixed N also increases.

The above analysis is applicable only for diffusive coupling through all substrates (all-component coupling). If we are interested in the stability of the CS state for a general symmetric coupling and for coupling only through end product (z) diffusion, we need to solve the master stability equation in eq. (11). In fig. 4(A), λ_{max} of the transverse manifold is shown for all-component coupling (left column), and z -component coupling (right column) as a function of α (which in turn involves both coupling strength ϵ and system size N). It is seen that λ_{max} becomes negative at $\alpha = -0.004$, and it remains negative as α becomes more negative. This entire range of α where λ_{max} is negative is the stability region for symmetric all-component coupling. The above analysis is valid for a general symmetric coupling matrix whose eigenvalues are parameterized by α . For a specific symmetric coupling matrix, the multi-cell system has a stable synchronized state if all the eigenvalues of its coupling matrix lie in the stable region. Next, we consider the z -component coupling (fig. 4(A) (right column)). Here, λ_{max} becomes negative only at $\alpha = -0.047$, and a larger coupling strength is required to attain the stability of the synchronized state. Thus there is a larger region of stability of the synchronized state for coupling through all components in comparison to coupling through the z component alone.

In order to recast this stability condition in terms of ϵ and N , we need to specialize to nearest-neighbor diffusive coupling where we can explicitly compute α as a function of ϵ and N . We obtain α by comparing eq. (8) with eq. (11). This gives $\alpha = -2\epsilon \sin^2 \frac{\pi k}{N}$. To obtain the largest transverse Lyapunov exponent, we set $k=1$, substitute this value of α in eq. (11). We numerically solve it to obtain

λ_{max} as a function of ϵ and N , for both all-component and z -only couplings. Figure 4(B) shows the variation of λ_{max} with ϵ for $N = 25$, 50, and 100. The left column in this figure is for all-component coupling, and the right column is for z -component coupling. First, we consider diffusion through all components. The left column of fig. 4(B)((i) and (ii)) illustrates that the ϵ value at which λ_{max} becomes negative increases as N increases: $\epsilon \approx 0.11$ for $N = 25$ and $\epsilon \approx 0.406$ for $N = 50$. This implies that a higher coupling strength is needed for the stability of the synchronized state for larger system sizes. For a larger multi-cellular system ($N > 82$), the synchronized state is unstable for all values of ϵ when the diffusive all-component coupling is considered. This is seen from fig. 4(B)(iii) (left column) for $N = 100$, where λ_{max} never becomes negative. This agrees with an earlier study on other systems [16] where the synchronized state for nearest-neighbor coupling was found to be unstable beyond a certain critical system size. The plots in the right column of fig. 4(B) show the results for the z -component coupling for different N values. Here λ_{max} never becomes negative for any ϵ , implying that the synchronized state is not stable for this range of coupling strength. The above results show the important role of the coupling topology on the stability of the emergent synchronized state.

There are a few features that have not been considered in this study. A topology, where all cells are coupled to all others (global coupling), is not commonly found in planar tissues. But other studies [3] have shown the stability region to be much bigger in such cases. As has been shown in other systems [17], this analysis can also be generalized to two-dimensional lattices. A preliminary study [8] showed that cells with small heterogeneity in parameters can still exhibit CS in the lattice. However, a comprehensive analysis of this system, incorporating the biologically realistic features of heterogeneity and noise, requires further study and will be addressed in future.

Discussion. Cell-to-cell communication is crucially important for development and maintenance of the integrity of structure and function in multi-cellular organisms. Nature uses a diversity of coupling mechanisms to enforce communication among cells in a cellular ensemble. A common mode of intercellular signaling couples the biochemical reaction pathways within each cell through diffusion of the products of these reactions. Such interactions influence the metabolically coupled cells to synchronize their inherent dynamics, which help coordinate and control their specific functions (normal and pathological) [18]. Synchronization is a widely studied phenomena in coupled nonlinear systems. In contrast to most earlier investigations that concentrated on synchronization of different types of biological oscillators [2,14,15,19], in this work, in addition to the role of system size and connection strength, we have also analyzed the differential role of the connection topology of intercellular interactions in the stability of the global synchronized state of the system.

A distinctive feature of this coupled cell system is that its collective behavior can be quite different from its constituent cells. Depending on the size of the multi-cellular system and coupling strength between the cells, the inherent chaotic dynamics of the constituent cells can remain chaotic or change to regular oscillations on coupling. Variation in the interaction strength can yield different types of synchronized states in the same system —completely synchronized, phase synchrony or intermittently synchronous dynamics. This is observed in living systems also where diverse mechanisms of intercellular exchange of information have been documented, and variation in strength of communication has been implicated in changes in dynamical states, some times leading to disease [20].

We have specifically studied two types of inter-cellular interactions —diffusion of all three components of the pathway, and only through the end product. We have shown that both types of interactions for the nearest-neighbor coupling can lead to the complete synchronization of dynamics in the multi-cellular system. But complete synchronization occurs for larger ranges of the system size (N) and connection strength (ϵ) when all components are interacting, and the synchronized state is stable for considerably large N for higher ϵ . However, the synchronized state is never stable for the end product coupled multi-cell systems for any N or ϵ . This is both surprising and interesting. It is expected that when more components of the same pathway are coupled, robust complete synchronization may occur for larger system size and lower interaction strength. But the complete absence of stability of the synchronized state for the end product coupled system indicates that, such a multi-cell system possesses the potential to induce transient or long-term changes in functional states in response to external stimuli —a feature seen during the development or initiation of a diseased state [6]. In biological systems, the most prevalent intercellular coupling is through the function-specific signaling molecules that generally occur as the end product of cascades of reactions. Such interactions with other cells induce gene expression, differentiation and other collective activities [21]. Thus, our theoretical study, on a simple model multi-cell system, provides clues that the coupling topology has an important role to play in the stability of the emergent functional state, and offer a physical basis to the prevalence of a certain type of coupling topology in multi-cellular systems. This furthers our general understanding of how multi-cellular systems implement collective robustness/sensitivity in a noisy world to perform their functions appropriately.

GR thanks DST Centre for Mathematical Biology and UGC-SAP at IISc, and is associated with the JNCASR, Bangalore. SS thanks Santa Fe Institute, USA, for visit under Senior International Fellowship. The authors thank the anonymous reviewers for giving valuable suggestions.

REFERENCES

- [1] LEVIN SIMON A., *PLoS Biol.*, **4** (2006) 1471.
- [2] PIKOVSKY A., ROSENBLUM M. and KURTHS J., *Synchronization: A Universal Concept in Nonlinear Sciences* (Cambridge University Press, Cambridge) 2001; ARENAS A., DÍAZ-GUILERA A., KURTHS J., MORENO Y., ZHOU C. and HAN S. K., *Phys. Rep.*, **469** (2008) 93.
- [3] CHEN Y., RANGARAJAN G. and DING M., *Phys. Rev. E*, **67** (2003) 026209.
- [4] RANGARAJAN G. and DING M., *Phys. Lett. A*, **296** (2002) 204.
- [5] PECORA L. M. and CARROLL T. L., *Phys. Rev. Lett.*, **80** (1998) 2109.
- [6] KANDLER K. and KATZ L. C., *Curr. Opin. Neurobiol.*, **5** (1995) 98; FOX JOHN E., BIKSON M. and JEFFERYS JOHN G. R., *J. Neurophysiol.*, **92** (2004) 181.
- [7] SINHA S. and RAMASWAMY R., *BioSystems*, **20** (1987) 341.
- [8] SUGUNA C. and SINHA S., *Physica A*, **346** (2005) 154.
- [9] GOLBETER A., *Biochemical Oscillations and Cellular Rhythms* (Cambridge University Press, Cambridge) 1996; GOLBETER A. and NICOLIS G., *Prog. Theor. Biol.*, **4** (1976) 65; GOODWIN B. C., *Analytical Physiology of Cell and Developing Organisms* (Academic Press, London) 1976; TYSON J. J., *J. Theor. Biol.*, **103** (1983) 313.
- [10] SUGUNA C., CHOWDHURY KANCHAN K. and SINHA S., *Phys. Rev. E*, **60** (1999) 5943.
- [11] SUGUNA C. and SINHA S., *Fluct. Noise Lett.*, **2** (2002) L313.
- [12] KOSEKA A., VOLKOV E., ZAIKIN A. and KURTHS J., *Phys. Rev. E*, **75** (2007) 031916.
- [13] WOLF A., SWIFT J. B., SWINNEY H. L. and VASTANO J. A., *Physica D*, **16** (1985) 285.
- [14] GARCIA-OJALVO J., ELOWITZ M. B. and STROGATZ S. H., *Proc. Natl. Acad. Sci. U.S.A.*, **101** (2004) 10955.
- [15] RAJESH S., SINHA S. and SINHA S., *Phys. Rev. E*, **75** (2007) 011906.
- [16] PALANIYANDI P. and RANGARAJAN G., *Phys. Rev. E*, **76** (2007) 027202.
- [17] RANGARAJAN G., CHEN Y. and DING M., *Phys. Lett. A*, **310** (2003) 415.
- [18] GUST J., WRIGHT J. J., PRATT E. B. and BOSMA M. M., *J. Physiol.*, **550** (2003) 123; MILLER M. B. and BASSLER B. L., *Annu. Rev. Microbiol.*, **55** (2001) 165; FREEMAN M. and GURDON J. B., *Annu. Rev. Cell Dev. Biol.*, **18** (2002) 515; JIRUSKA P., CSICSVARI J., POWELL A. D., FOX J. E., CHANG W., VREUGDENHIL M., LI X., PALUS M., BUJAN A. F., DEARDEN R. W. and JEFFERYS J. G. R., *J. Neurosci.*, **30** (2010) 5690.
- [19] NGUYEN C. and HAN S. K., *EPL*, **90** (2010) 10010.
- [20] FOX J. E., BIKSON M. and JEFFERYS J. G. R., *J. Neurophysiol.*, **92** (2004) 181; LIEBNER S., CAVALLARO U. and DEJANA E., *Arterioscler. Thromb. Vasc. Biol.*, **26** (2006) 1431; PANFILOV A. V., *Phys. Rev. Lett.*, **88** (2002) 118101; PEERCY B. E. and KEENER J. P., *SIAM J. Appl. Dyn. Syst.*, **4** (2005) 679; GIURUMESCU C. A., STERNBERG P. W. and ASTHAGIRI A. R., *Proc. Natl. Acad. Sci. U.S.A.*, **103** (2006) 1331.
- [21] LODISH H., BERK A., ZIPURSKY S. L., MATSUDAIRA P., BALTIMORE D. and DARNELL J., *Molecular Cell Biology*, 4th edition, (W. H. Freeman, New York) 2000, Chapt. 20: *Cell-to-Cell Signaling: Hormones and Receptors*.